

## Accepted Manuscript

Spatial Correlation as an Early Warning Signal of Regime Shifts in a Multiplex Disease-Behaviour Network

Peter C. Jentsch, Madhur Anand, Chris T. Bauch

PII: S0022-5193(18)30140-1  
DOI: [10.1016/j.jtbi.2018.03.032](https://doi.org/10.1016/j.jtbi.2018.03.032)  
Reference: YJTBI 9409



To appear in: *Journal of Theoretical Biology*

Received date: 9 May 2017  
Revised date: 12 February 2018  
Accepted date: 19 March 2018

Please cite this article as: Peter C. Jentsch, Madhur Anand, Chris T. Bauch, Spatial Correlation as an Early Warning Signal of Regime Shifts in a Multiplex Disease-Behaviour Network, *Journal of Theoretical Biology* (2018), doi: [10.1016/j.jtbi.2018.03.032](https://doi.org/10.1016/j.jtbi.2018.03.032)

This is a PDF file of an unedited manuscript that has been accepted for publication. As a service to our customers we are providing this early version of the manuscript. The manuscript will undergo copyediting, typesetting, and review of the resulting proof before it is published in its final form. Please note that during the production process errors may be discovered which could affect the content, and all legal disclaimers that apply to the journal pertain.

1 **Highlights**

- 2     • A two-layer network simulation model of disease spread and vaccinating  
3       behaviour is developed.
- 4     • Early warning signals of a regime shift in vaccinating behaviour are  
5       explored.
- 6     • Early warning signals are identified in four of the five network topologies  
7       studied.

ACCEPTED MANUSCRIPT

8 Spatial Correlation as an Early Warning Signal of  
9 Regime Shifts in a Multiplex Disease-Behaviour  
10 Network

11 Peter C. Jentsch<sup>a,b</sup>, Madhur Anand<sup>b</sup>, Chris T. Bauch<sup>\*a</sup>

12 <sup>a</sup>*Department of Applied Mathematics, University of Waterloo, 200 University Avenue*  
13 *West, Waterloo, Ontario, Canada N2L 3G1. \*cbauch@uwaterloo.ca*

14 <sup>b</sup>*School of Environmental Sciences, University of Guelph, 50 Stone Road East, Guelph,*  
15 *Ontario, Canada N1G 2W1.*

---

16 **Abstract**

Early warning signals of sudden regime shifts are a widely studied phenomenon for their ability to quantify a system's proximity to a tipping point to a new and contrasting dynamical regime. However, this effect has been little studied in the context of the complex interactions between disease dynamics and vaccinating behaviour. Our objective was to determine whether critical slowing down (CSD) occurs in a multiplex network that captures opinion propagation on one network layer and disease spread on a second network layer. We parameterized a network simulation model to represent a hypothetical self-limiting, acute, vaccine-preventable infection with short-lived natural immunity. We tested five different network types: random, lattice, small-world, scale-free, and an empirically derived network. For the first four network types, the model exhibits a regime shift as perceived vaccine risk moves beyond a tipping point from full vaccine acceptance and disease elimination to full vaccine refusal and disease endemicity. This regime shift is preceded by an increase in the spatial correlation in non-vaccinator opinions beginning well before the bifurcation point, indicating CSD. The early warning signals occur across a wide range of parameter values. However, the more gradual transition exhibited in the empirically-derived network underscores the need for further research before it can be determined whether trends in spatial correlation in real-world social networks represent critical slowing down. The potential upside of having this monitoring ability suggests that this is a worthwhile area for further research.

17 *Keywords:* adaptive networks, multiplex networks, behavioral modelling,

18 coupled behavior-disease models, regime shifts, early warning signal

---

## 19 1. Introduction

20 Vaccine-preventable infectious diseases continue to impose significant bur-  
21 dens on populations around the world [1]. Access to vaccines remains a sig-  
22 nificant barrier to providing more widespread protection against infectious  
23 diseases. However, a growing obstacle to infection control is vaccine refusal,  
24 which can have a large effect on disease prevalence. For instance, the drop  
25 in vaccine coverage after Andrew Wakefield’s fraudulent 1998 paper about  
26 the mumps-measles-rubella vaccine reduced MMR coverage to as low as 61  
27 % in some areas of the United Kingdom [2]. Lower vaccine coverage caused  
28 larger measles outbreaks in the years following the publication of the Wake-  
29 field paper [3][4]. Elimination of polio in Africa was similarly interrupted  
30 when a rumor that the vaccine could cause infertility or HIV infection began  
31 spreading in 2003, when leaders of three states in north-central Nigeria boy-  
32 cotted the vaccine until it could be tested independently. The impasse was  
33 not resolved until the following year, a time period during which these states  
34 accounted for over 50% of polio cases worldwide [5, 6]. Vaccine refusal and  
35 hesitancy are also common for influenza vaccine, with non-vaccinators citing  
36 concern for side effects, lack of perception of infection risk, and doubts about  
37 vaccine efficacy as reasons to not become vaccinated [7].

38 Simple differential equation models such as the Kermack-McKendrick SIR  
39 (susceptible-infected-recovered) model published in 1927 (originally formu-  
40 lated as an integro-differential equation) [8], allow us to characterize useful  
41 measures such as the expected number of new infections caused by each in-  
42 fection, and are readily fitted to epidemiological data. Classical infection  
43 transmission models such as the Kermack-McKendrick model assume that  
44 members of the population mix homogeneously. However, in many situa-  
45 tions, infection transmission through a network—where individuals are nodes  
46 and contacts through which infection may pass are edges—are a more accu-  
47 rate description of infection dynamics [9]. Networks tend to be analytically  
48 intractable and therefore agent-based models are often used to simulate net-  
49 works. Agent-based simulations on networks allow us to specify complex in-  
50 dividual node behavior in a natural way. One of the most ambitious examples  
51 of these is the Global-Scale Agent Model, which models the daily behavior  
52 and relationships of 6.5 billion people using worldwide GIS data[10]. How-  
53 ever, agent-based network simulations have also been studied in the context

54 of nonlinear interactions between disease dynamics and individual behaviour  
55 concerning vaccines and contact avoidance [11, 12, 13, 14, 15].

56 The trajectory that an infection takes as it moves through a population is  
57 heavily influenced by the spread of health information between individuals, so  
58 more sophisticated models of disease spread often combine disease dynam-  
59 ics and social dynamics. The coupled interactions between individual be-  
60 haviour and disease dynamics have been modelled under various frameworks  
61 and placed under various rubrics including: epidemic games [16], coupled  
62 behaviour-disease models [12, 17, 18], socio-epidemiology, economic epidemi-  
63 ology and behavioural modeling [19]. . A more recent trend in epidemio-  
64 logical modeling is to abstract these two subsystems into (1) an information  
65 transfer network through which information flows between individuals, and  
66 (2) a separate physical disease transmission network. A system where each  
67 node is part of two or more different networks is called a multiplex net-  
68 work, and is a natural way to implement a coupled disease-behaviour system  
69 [20, 18]. For instance, the simultaneous spread of disease and disease aware-  
70 ness over adaptive multiplex networks with scale-free degree distributions  
71 has been studied [21]. Similarly, a three layer network to model the diffusion  
72 of infection, awareness, and preventative measures along different contact  
73 networks was found to reasonably approximate empirical influenza data[22].  
74 Similar approaches consider coupled human and ecological dynamics, which  
75 present the opposite problem of species that humans wish to preserve instead  
76 of eradicate [23, 24, 25, 26].

77 The nonlinear coupling between disease and social processes creates feed-  
78 back loops between infection prevention mechanisms and disease spread.  
79 Nonlinear feedback in other complex systems such as from solid state physics  
80 and theoretical socio-ecology has often been shown to yield critical transitions  
81 [27, 28, 26]. A critical transition is defined as an abrupt shift from an exist-  
82 ing dynamical regime to a strongly contrasting (and sometimes unfavourable)  
83 dynamical regime as some external parameter is pushed past a bifurcation  
84 point [29, 30]. Fortunately, critical transitions (and other regime shifts as-  
85 sociated with a bifurcation where the **dominant eigenvalue of the Jacobian**  
86 matrix around the equilibrium approaches zero) often exhibit characteris-  
87 tic early warning signals beforehand that allow these shifts to be predicted  
88 [31, 32, 30]. Critical slowing-down (CSD) based indicators were one of the  
89 first early warning signals to be studied. CSD occurs because the speed with  
90 which a system responds to perturbations slows as it approaches bifurcations  
91 where the magnitude of the dominant eigenvalue of the Jacobian approaches

92 zero at the bifurcation point. Since nearly all systems in the real world are  
93 subject to perturbations, the lag-1 autocorrelation of a time series can be  
94 used as a relatively universal (or at least potentially common) indicator of  
95 CSD. Lag-1 autocorrelation appears to be a robust statistic and has been  
96 shown to be present in predicting catastrophic bifurcations in complex real  
97 world systems such as the global climate[33], human nervous systems[34],  
98 and stock markets[35].

99 The discrete fourier transform (DFT) of a network is another example  
100 of a CSD-based early warning signal. Under some assumptions, the Weiner-  
101 Kinchin Theorem shows that we can use the discrete Fourier transform (DFT)  
102 to measure spatial correlation in system state, and this has been shown to  
103 work in some ecological applications [36] [37]. Lag-1 spatial correlation can in  
104 some cases provide a better early warning signal than time-domain methods,  
105 because "a spatial pattern contains much more information than does a single  
106 point in a time series, in principle allowing shorter lead times" before the  
107 critical transition occurs [38, 31]. This observation has been corroborated in  
108 three ecological dynamical systems[31].

109 Early warning signals of regime shifts in coupled behaviour-disease net-  
110 works have received relatively little attention in the literature on modelling  
111 interactions between disease dynamics and human behaviour. This appears  
112 to be a significant knowledge gap because early warning signals for vaccine  
113 scares could help public health anticipate widespread vaccine refusal and  
114 prepare for outbreak response in advance, as well as build efforts to improve  
115 trust between the public and the health authorities. In this paper we use an  
116 agent-based model on a two-layer multiplex network to simulate the coupled  
117 disease dynamics of a vaccine-preventable infection and social dynamics of  
118 vaccination in a population. We show that spatial correlation can be used as  
119 an early warning signal for regime shifts in this system on most (but not all)  
120 network topologies. In the next section we discuss the model structure and  
121 methods of analysis, followed by a section on results and finally a discussion  
122 section.

## 123 2. Methods

### 124 2.1. Simulation

125 Our agent-based model simulated a population of 10,000 individuals (nodes),  
126 where every node belongs to two different connectivity networks: a transmis-  
127 sion network and a social network. In the transmission network, each node

128 is connected to other nodes from which they can contract infection. Two  
 129 nodes are linked in the social network if they can be influenced by one an-  
 130 other's opinions on vaccination. These networks were simulated as fixed  
 131 graphs upon which stochastic processes occurred, with a variety of degree  
 132 distributions and average path lengths.

133 We modelled a hypothetical acute, self-limiting infection with rapidly  
 134 waning natural immunity. Each node on the physical layer is in one of four  
 135 possible states: susceptible ( $S$ ), infected ( $I$ ), recovered ( $R$ ), or vaccinated  
 136 ( $V$ ). Each node on the social layer also has an opinion on the vaccine: they  
 137 are either a non-vaccinator ( $\eta$ ), or a vaccinator ( $\nu$ ). We will denote the  
 138 biological state of a node  $v$  by  $B(v)$ , and the opinion of a node  $v$  by  $\Theta(v)$ .  
 139 The transmission network is a graph denoted by  $T(V, E_T)$ , and the social  
 140 network is a graph denoted by  $O(V, E_O)$ . We assume that they share the  
 141 same set of vertices  $V$  although this assumption could be relaxed in future  
 142 work. The set of nodes in the neighbourhood of  $v$  is  $adj_T(v)$  or  $adj_O(v)$  for  
 143 the transmission and the social network respectively.

144 The algorithm used to simulate the social and transmission processes used  
 145 discrete timesteps. At each time step, for each  $v \in V$ :

- 146 • If  $B(v) = I$ , then for all  $u \in adj_T(v)$  such that  $B(u) = S$  and  $\Theta(u) \neq \nu$ ,  
 147 set  $B(u) = I$  with probability  $p$  (infection event)
- 148 • If  $B(v) = I$ , let  $B(v) = R$  with probability  $r$  (natural recovery event)
- 149 • If  $B(v) = R$ , set  $B(v) = S$  with probability  $\gamma$  (loss of immunity event)
- 150 • If  $B(v) = S$ , set  $B(v) = I$  with probability  $\sigma \ll 1$  (case importation  
 151 event)
- 152 • Choose some node  $u \in adj_O(v)$  uniformly at random. If  $\Theta(v) \neq \Theta(u)$ ,  
 153 then  $P(\eta \rightarrow \nu) = \Phi(E_V - E_N)$ , and  $P(\nu \rightarrow \eta) = 1 - \Phi(E_V - E_N)$   
 154 where

$$155 \quad E_V = -c_v + c_n, \quad (1)$$

$$E_N = -c_I \mathfrak{J}(v), \quad (2)$$

156 where  $\Phi$  is a sigmoid function such that  $\Phi(\infty) = 1$ ,  $\Phi(-\infty) = 0$ ,  
 157  $\Phi(0) = 0.5$  as described in previous models (opinion change event)  
 158 [39]. In our implementation,  $\Phi(x) = \frac{1}{1+e^{-\beta x}}$ ,  $c_v$  is the perceived cost of

159 vaccination (due to infection risks),  $c_I$  is the perceived cost of infection  
 160 (due to infection risks),  $\beta$  controls the steepness of the sigmoid function,  
 161 and  $\mathfrak{J}(v) = |\{u \in \text{adj}_T(v) : B(u) = I\}|$  is the number of infected nodes  
 162 adjacent to  $v$  in the transmission network.  $c_n$  represents some outside  
 163 incentive that a person might have for vaccinating, such as peer ap-  
 164 proval, school admission requirements, or tax incentives. Normalizing  
 165 both payoff equations by  $c_I$  yields

$$166 \quad E_V = -c + \xi \quad (3)$$

$$167 \quad E_N = -\mathfrak{J}(v) \quad (4)$$

167 where  $c$  is the ratio of perceived vaccine risk to perceived disease risk,  
 168 and  $\xi = \frac{c_n}{c_I}$  is the ratio of the vaccination incentive to the perceived  
 169 disease risk. Since changes in perceived vaccine risk are controlled  
 170 through changes in  $c$ , we will vary  $c$  in our analysis. We assume the  
 171 vaccine is perfectly efficacious.

- 172 • With probability  $\epsilon$ ,  $v$  changes opinions (random opinion change event).  
 173 That is, if  $\Theta(v) = \nu$ , set  $\Theta(v) = \eta$  and vice-versa.
- 174 • If the opinion of a node changes to vaccinator, then their physical state  
 175 changes to immunized immediately. If they change back to a non-  
 176 vaccinator, they become susceptible immediately.

177 We applied synchronized updating to the network: the change in state re-  
 178 sulting from each rule is stored and applied after every rule is checked, so  
 179 the order of the above steps does not matter.

180 The result of these rules is a feedback loop where, depending on the rel-  
 181 ative costs of vaccination and infection, the population tends not to exhibit  
 182 a mixture of strategies except near the critical values of  $c$ . When  $c < \xi$ , the  
 183 payoff to vaccinate  $E_V$  is positive and thus exceeds the payoff not to vacci-  
 184 nate  $E_N$  which always obeys  $E_N \leq 0$ . In this case, in the limit as  $\beta \rightarrow \infty$ , all  
 185 nodes are therefore vaccinators and the infection dies out. However, when  
 186  $c > \xi$  and thus  $E_V < 0$ , the disease-free equilibrium destabilizes since  $E_N \approx 0$   
 187 in the absence of sustained transmission. In general, since the vast major-  
 188 ity of nodes do not have infected neighbours at the disease-free equilibrium,  
 189 there is a rapid shift in the population to non-vaccinator opinions as well  
 190 as epidemic outbreaks. For larger values of  $\beta$ , the function controlling the  
 191 opinion-switching as a function of the payoff difference between vaccinator



192 and non-vaccinator strategies is steeper, and the population transition from  
 193 non-vaccinator to vaccinator strategies is therefore sharper, yielding a crit-  
 194 ical transition. However, we will use the more general term ‘regime shift’  
 195 throughout this paper, since the transition can be made more or less abrupt  
 196 by changing the value of  $\beta$ .

## 197 2.2. Early Warning Signal Analysis

198 As the system approaches a regime shift, the dominant eigenvalue of  
 199 the underlying dynamical system will approach zero. Therefore, it will take  
 200 longer for the system to recover from perturbations to the steady state. In  
 201 a spatially extended population, this will increase population heterogeneity  
 202 as small clusters of non-vaccinators begin to emerge, as well as causing long-  
 203 range correlations to develop across the network in a detectable way [31].  
 204 This development is reflected by an increase in a statistic called the lag-1  
 205 spatial correlation (lag-1 SC). We used Moran’s I to measure the lag-1 SC  
 206 of non-vaccinators as described in [40]. Moran’s I is widely used to calculate  
 207 the spatial correlation for early warning signals [41, 42, 43].

208 Let  $G = (V, E)$  be a graph with  $n$  nodes,  $adj(v)$  be the set of vertices  
 209 adjacent to  $v$ , and  $f(v)$  be a binary function such that  $f(v) = 1$  if  $v$  is a  
 210 vaccinator, and  $f(v) = 0$  otherwise. We define Moran’s I at lag-1, called  $M$   
 211 to prevent confusion with the Infected state, as:

$$M = \frac{\sum_{v \in V} I_v}{|E|} \quad (5)$$

$$M_v = \frac{n(f(v) - \bar{x}) \sum_{w \in adj(v)} (f(w) - \bar{x})}{\sum_{w \in V} (f(w) - \bar{x})^2} \quad (6)$$

212 where  $\bar{x} = \frac{1}{n} \sum_{v \in V} f(v)$  is the fraction of vaccinators in the network. Far  
 213 from the regime shift, we have that  $\bar{x} \approx 1$  and  $f \approx 1$  for all nodes, thus  
 214  $I \approx 0$ . However, as resilience to perturbations declines close to the regime  
 215 shift, the population become more heterogeneous. This causes  $f - \bar{x} \approx -1$   
 216 in correlated non-vaccinator clusters, thus  $I$  increases.

217 For each realization, the simulation was run long enough for the spatial  
 218 correlation to stabilize (3500 timesteps), and the equilibrium value was cal-  
 219 culated as the average of the next 500 measurements. The equilibrium lag-1  
 220 SC was obtained for 100 realizations of the simulation, and these values were  
 221 averaged to obtain a data point for every value of  $c$ . The social network  
 222 and the transmission network are always both the same type of network, but  
 223 independently generated.

Parameter	Value	Definition
$p$	0.5	Probability that an infected node infects a given susceptible neighbour
$r$	0.07143	Probability that an infected node recovers
$\gamma$	0.001369	Probability that a recovered node becomes susceptible
$\epsilon$	0.001369	Probability that a node randomly switches their opinion on vaccination
$\sigma$	0.016666	Probability of disease reintroduction
$\xi$	0	Parameter governing incentive to become vaccinated
$c$	0.1	Ratio of perceived risk of vaccine to perceived risk of disease
$\beta$	1	Parameter controlling the steepness of $\Phi$

Table 1: Parameter definitions and baseline parameter values in probability per timestep (unless otherwise stated). One timestep was interpreted to correspond to one day.

### 2.3. Parameter Values

Baseline parameter values appear in Table 1. The parameter values were chosen to qualitatively represent a hypothetical acute-self limiting infection with waning natural immunity, such as the case of meningococcal infection, influenza or pertussis [44, 45, 46, 47]. The value for  $r$  corresponds to a mean duration of infection of 14 days, the value for  $\gamma$  corresponds to losing natural immunity after two years, and the value for  $\sigma$  corresponds to a case importation event in the network once every two months. We conduct univariate sensitivity analysis with respect to  $r$  and  $\sigma$ , since they are important parameters governing the natural history of the infection. For the baseline parameter values,  $\xi$  is set to zero without loss of generality. The value of  $c$  will be varied in the analysis of early warning signals.  $\epsilon > 0$  is required to prevent the population from fixating on one of the two strategies. To initialize each stochastic realization, one randomly chosen node is infected, and each node is a vaccinator with probability 0.5.

### 2.4. Networks

We ran our model on five different networks: Erdos-Renyi [48], Barabasi-Albert [49], square lattice (or grid), Kleinberg small world[50], and ten subsets of a network constructed by the Network Dynamics and Simulation and

243 Science Laboratory (NDSSL), based on GIS data from the city of Portland  
 244 [51].

245 An Erdos-Renyi network is simply given a set of nodes  $V$  and  $v, w \in V$ ,  
 246  $v$  is connected to  $w$  with some probability  $p$ . In our Erdos-Renyi network  
 247 model, we used a connection probability of 0.001, so each node has degree  
 248 10 on average.

249 The Barabasi-Albert model yields networks with a scale-free (or power-  
 250 law) node degree distribution. Starting with a small initial connected network  
 251  $(V, E)$ , new nodes are added to  $V$  one at a time. Where the probability that  
 252 the new node is connected to an existing node  $v \in V$  is  $p_v = \frac{\text{deg}(v)}{\sum_{w \in V} \text{deg}(w)}$ . To  
 253 ensure that the network is always connected, new nodes are also connected  
 254 to  $m$  existing vertices, chosen uniformly at random. The Barabasi-Albert  
 255 networks we used had  $m = 1$ .

256 Our lattice with  $n = 10,000$  nodes was built as follows: if the nodes  
 257 are arranged on the integer points of a square  $\sqrt{n}$  units wide, each node is  
 258 connected to the nodes within a unit distance up or down (but not both).  
 259 Because lattice networks are not random, there is no difference between the  
 260 social and transmission networks and therefore this is effectively not a mul-  
 261 tiplex network.

262 The Kleinberg small world network is defined as a square lattice, where  
 263 additional edges are added between some nodes  $v$  and  $w$  with a probability  
 264 proportional to  $1/d(v, w)$ . The result of this process is a network with a very  
 265 short average path length. In our implementation, nodes only gain extra  
 266 edges with 0.1 probability.

267 The empirically-derived networks from the NDSSL dataset are designed to  
 268 have some of the properties of a real contact network, being derived from the  
 269 population of Portland, Oregon. We used a set of ten subnetworks sampled  
 270 from the NDSSL dataset and constructed in such a way to share the same  
 271 properties as the original dataset (see Ref. [39] and supplementary appendix  
 272 for details). The subnetworks had an average path length of  $4.020 \pm 0.126$ ,  
 273 and an average clustering coefficient of  $0.747 \pm 0.006$ . For each run, two  
 274 networks were chosen from the 10 networks uniformly at random and one  
 275 was set as the social network, with the other as the transmission network.

### 276 3. Results

#### 277 3.1. Model dynamics

278 We generated time series of the percentage of vaccinators and percent-  
 279 age of infected persons for each of the networks, in order to illustrate the  
 280 basic dynamics exhibited by the model. We used baseline parameter values  
 281 everywhere (Table 1) except that  $c = 0.3$ . For all networks we initialized  
 282 the population to have a low initial number of vaccinators and a large initial  
 283 number of susceptible persons. These initial conditions caused the incidence  
 284 of infection to skyrocket at the beginning of the simulation for all network  
 285 types (Figure 1). Immediately after this initial outbreak, susceptible neigh-  
 286 bours of infected persons get vaccinated, thereby reducing prevalence.

287 After this initial spike, the dynamics settle down into pseudo-stable pat-  
 288 terns that vary widely depending on network type. More frequent outbreaks  
 289 appear to occur on networks with higher degree, which is consistent with intu-  
 290 ition (Figure 1). The random network exhibits relatively regular outbreaks  
 291 (Figure 1a), while the square lattice, Barabasi-Albert network, and small  
 292 world network exhibit more irregular dynamics consisting of large outbreaks  
 293 interspersed with periods of very low vaccine coverage and infection preva-  
 294 lence (Figure 1b-d). However, during certain phases in the time series, the  
 295 small-world network appears to transition to a regime of sustained endemic  
 296 infection similar to that observed for the random network (Figure 1d). The  
 297 empirically-derived network exhibits small stochastic fluctuations around an  
 298 equilibrium, and the percentage of vaccinators is significantly higher in the  
 299 empirically-derived network than in the other four networks (Figure 1e).

#### 300 3.2. Regime shifts

301 We carried out this simulation experiment for a range of values of  $c$  to  
 302 understand how dynamics respond to changes in the perceived vaccine risk  
 303  $c$ . We computed the long-term average prevalence of infected persons and  
 304 vaccinators for each value of  $c$  tested. As  $c$  approaches zero from below (for  
 305  $\xi = 0$ ), a transition from a regime of high vaccine coverage and low infection  
 306 prevalence to a regime of low vaccine coverage and endemic infection should  
 307 be observed, since for  $c > 0$ , the payoff to vaccinate becomes less than the  
 308 payoff not to vaccinate.

309 In the simulations we observe a transition in the percentage of non-  
 310 vaccinators as a function of the perceived vaccine risk  $c$  in most of the network  
 311 types (Figure 2). As  $c$  approaches zero, the prevalence of vaccinators declines

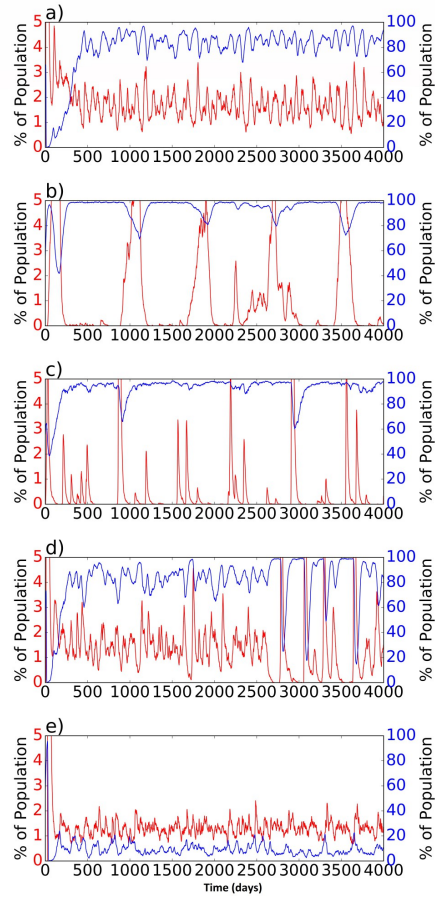


Figure 1: Time series for a typical simulation on each network type: a) random network, b) square lattice, c) Barabasi-Albert network, d) Small world network, e) empirically-derived networks. Red line is percentage of infected individuals in the population; blue line is percentage of vaccinators in the population. Parameter values are as in Table 1 except  $c = 0.3$ .

312 dramatically in the first four networks. The transition appears gradual (non-  
 313 critical) in the empirically-derived network (Figure 2e). We speculate this  
 314 is due to the greater heterogeneity exhibited by the empirically-derived net-  
 315 work than the other four idealized network types. The percentage of infected  
 316 persons in each network shows similar transitions, even in the latter network  
 317 (Figure 2e). We also note that the transition is sharper when the sigmoid  
 318 function used in decision-making is steeper (higher  $\beta$ ; results not shown).

### 319 3.3. Early warning signals

320 Indicators such as spatial correlation can signal an impending critical  
 321 transition in spatially structured ecological systems [31]. Although theo-  
 322 retical results are not available for coupled behaviour-disease dynamics on  
 323 multiplex networks, the universality of dynamics near local bifurcations of  
 324 dynamical systems [32] suggests that similar early warning signals should be  
 325 observed in our system.

326 In spatially extended critical phenomena, the plot of spatial correlation  
 327 versus a bifurcation parameter such as  $c$  is linear on a log-linear plot [52].  
 328 Hence, we computed the average lag-1 spatial correlation (SC) across the  
 329 entire time series. We repeated this for many values of  $c$  and plotted lag-1  
 330 AC versus  $c$  on a log-linear scale. As noted previously, we expect near the  
 331 threshold  $c = 0$  where the costs and benefits of the vaccine become balanced,  
 332 that critical slowing down should emerge in the network, and that this should  
 333 manifest as increased spatial correlation. As we increase  $c$  from negative to  
 334 positive, small clusters of non-vaccinators begin to appear. Each day every  
 335 node samples a random neighbour, and the only other way for that node to  
 336 switch opinions is if the randomly sampled neighbour has a different opinion  
 337 that they do (see Methods). As a result, we expect to see clusters of non-  
 338 vaccinators emerge, which causes the lag-1 SC to increase before the critical  
 339 transition (and after which almost everyone because a non-vaccinator) (figure  
 340 3).

341 This pattern is observed in simulations for all network types. As the  
 342 regime shift at  $c = 0$  is approached from negative values of  $c$  (corresponding  
 343 to a rise in perceived vaccine risks), we observe a clear and linear increase  
 344 in the time-averaged lag-1 SC, in plots of the natural logarithm of lag-1 SC  
 345 versus  $c$  (Figure 4). This is robust to values of the disease transmission  
 346 probability,  $p$  (Figure 4).

347 However, there is a notable difference in y-axis scales for the random and  
 348 small-world networks (Figure 4a,d). Overall these networks show a smaller

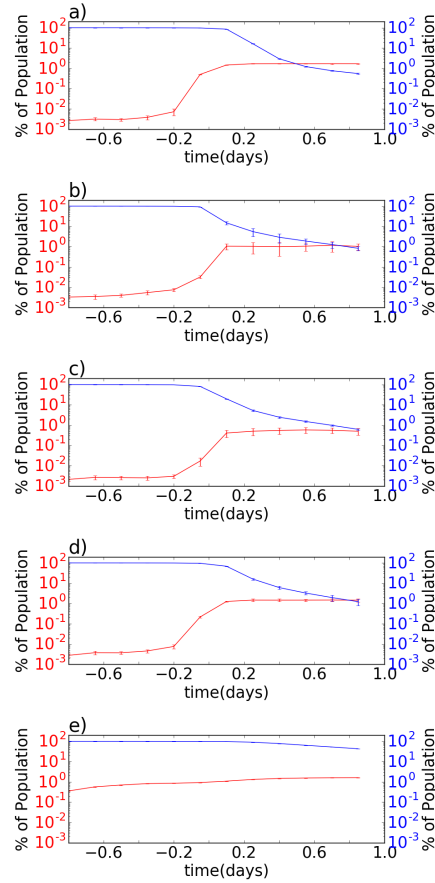


Figure 2: The time-averaged percentage of infected persons and vaccinators as a function of relative vaccine cost  $c$ , showing a critical transition near  $c = 0$  on the a) random network, b) square lattice, c) Barabasi-Albert network, d) Small world network, and a more gradual transition on the e) empirically-derived networks. All parameters are as in Table 1 except for  $c$ , which is being varied. The blue line represents the percentage of vaccinators, and the red line percentage of infected. Error bars represent the standard deviation over the 100 realizations.

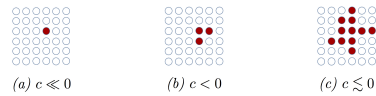


Figure 3: Visualization of non-vaccinator spatial correlation on a square lattice. As  $c$  approaches the critical transition at  $c = 0$ , clusters of non-vaccinators (red) begin to appear, increasing the spatial correlation of non-vaccinators.

349 increase in spatial correlation, possibly due to the smaller average path length  
 350 in these networks. Furthermore, lag-1 SC in the empirically-derived network  
 351 has a nonlinear and more gradual response to changes in  $c$ , which matches the  
 352 lack of a sharp critical transition in that network. Sensitivity analyses over  
 353  $r$  and  $\sigma$  confirm the same patterns, except in the extreme case of  $r = 0.02$   
 354 where infected individuals never recover (Figure 5).

355 We observe that the rise in the natural logarithm of lag-1 SC begins well  
 356 before the number of non-vaccinators begins to increase appreciably (com-  
 357 pare  $c \in [-0.8, -0.2]$  in Figure 4 versus Figure 2). Therefore, tracking lag-1  
 358 SC can provide an early warning signals of potential shifts in population vac-  
 359 cinating behaviour that would not be accessible simply by extrapolating the  
 360 number of non-vaccinators using a linear regression, for instance. Moreover,  
 361 this rise in lag-1 SC is highly robust to network type and parameter value,  
 362 due to the fundamental assumption that a node's vaccination status is influ-  
 363 enced by the opinions of the nodes in their social neighbourhood. However,  
 364 the location of the regime shift in  $c$  is related to the average node degree:  
 365 with an average node degree of 100, the regime shift occurs at approximately  
 366  $c = 2.4$ .

#### 367 4. Discussion

368 Here we studied regime shifts in coupled behaviour-disease dynamics on  
 369 a multiplex network where an infectious disease is transmitted through the  
 370 physical network layer, and the social layer describes a population where  
 371 everyone has either a pro-vaccine or an anti-vaccine opinion. These simu-  
 372 lation results show the presence of critical slowing down near a bifurcation  
 373 in the multiplex network corresponding to a switch from predominant vac-  
 374 cinating behaviour and disease elimination, to predominant non-vaccinating  
 375 behaviour and disease endemicity. Critical slowing down was clearly man-  
 376 ifested in all network types and across a broad range of parameter values,  
 377 with the exception of the empirically derived network. This exception may



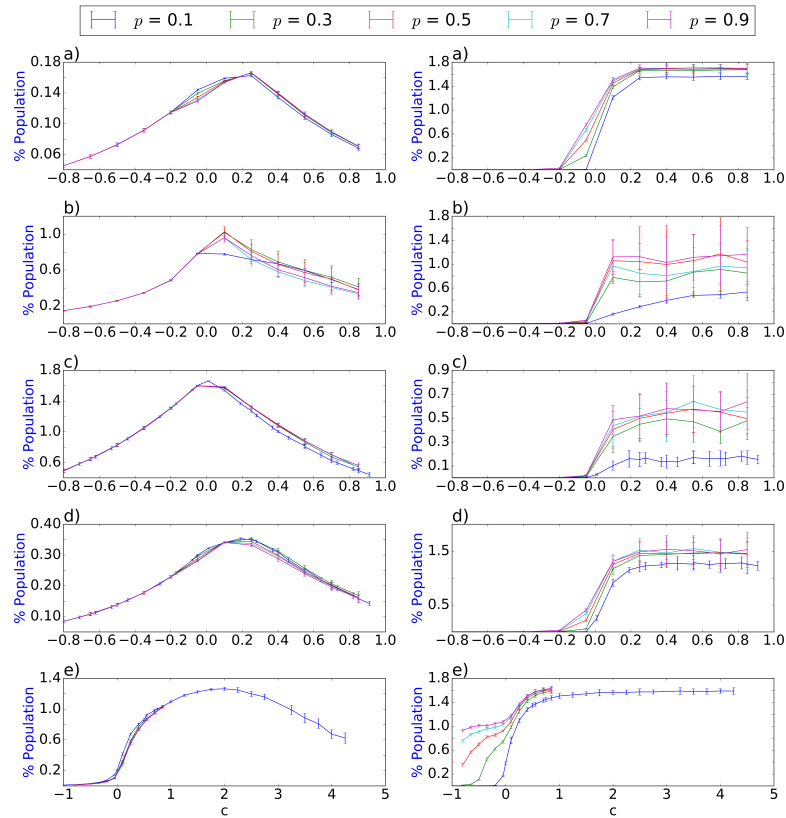


Figure 4: The natural logarithm of the time-averaged lag-1 SC of nonvaccinators, and the percentage of infected nodes, for a range of values of  $c$ , showing a linear increase in lag-1 SC in a log-linear plot as the critical transition is approached on a) random network, b) square lattice, c) Barabasi-Albert network, d) Small world network, e) empirically-derived networks. All other parameter values are as in Table 1.

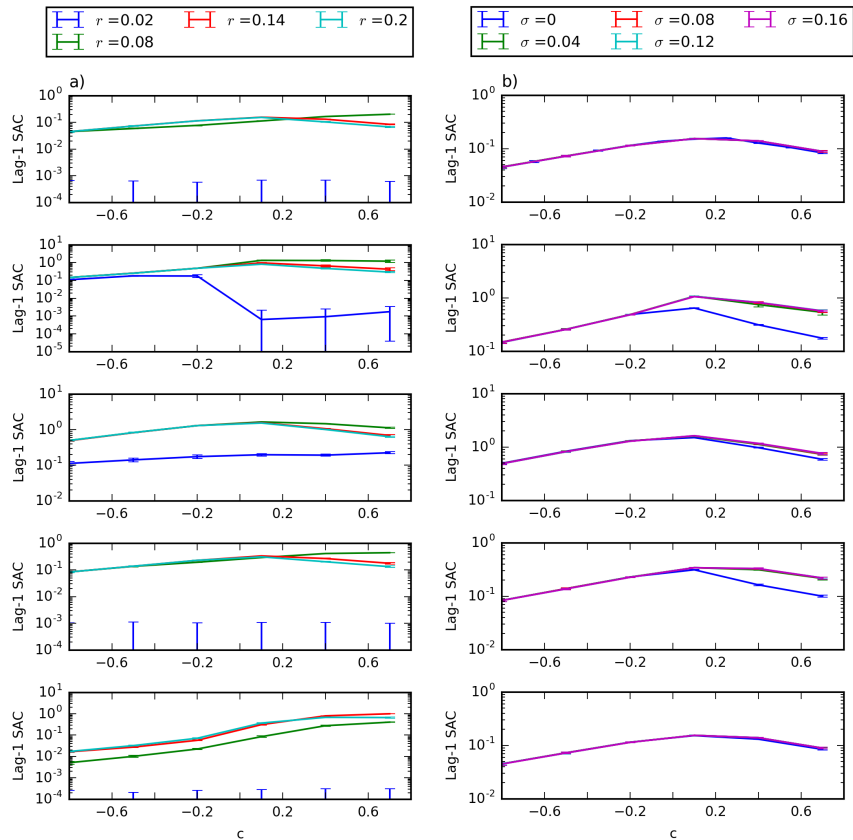


Figure 5: The natural logarithm of the time-averaged lag-1 SC of nonvaccinators for a range of values of  $c$  at selected values of a)  $r$  and b)  $\sigma$ , showing a linear increase in lag-1 SC in a log-linear plot as the critical transition is approached. Networks types from top row to bottom row are: random network, square lattice, Barabasi-Albert network, small world network, and empirically-derived networks. All parameters besides  $r$ ,  $\sigma$  and  $c$  are the same as Table 1.

378 have been on account of the greater heterogeneity of the **network structure**  
379 causing lack of a sharp transition to non-vaccinating behaviour.

380 Hence, the results suggest that it may be possible to use lag-1 spatial cor-  
381 relation in social networks as an early warning signal of widespread vaccine  
382 refusal in a population. However, the lack of a clear transition in the case of  
383 the network that was empirically derived (from NDSSL data) suggests that  
384 further research must be conducted in order to determine how and whether  
385 it would be possible to detect such early warning signals in real-world social  
386 networks, and what the trends in correlation indicators might signify. **We**  
387 **speculate that our approach might have failed for the empirical network due**  
388 **to multiple sources of heterogeneity in network structure such as: a highly**  
389 **dispersed node degree distribution; the presence of disconnected subgraphs;**  
390 **and/or differing network structure in different parts of the network. How-**  
391 **ever, it is possible that including peer pressure (social norms) in the model**  
392 **might cause population opinion states to shift to bistable boundary equilibria**  
393 **corresponding to all-vaccinator or no-vaccinator population compositions—as**  
394 **has been observed in other socio-ecological models—and thus restore the fea-**  
395 **sibility of early warning signals [26].** Our model also assumed that networks  
396 are static and that the two layers are perfectly correlated. Neither condition  
397 holds in real populations, and these simplifying assumptions could be relaxed  
398 in future work.

399 It is also possible to tailor this model to specific infectious diseases such as  
400 measles or influenza by modifying the model to include relevant vital dynam-  
401 ics, disease natural history, and vaccine characteristics. This is particularly  
402 important since disease natural history can have a significant impact on dis-  
403 ease dynamics [44, 53], and vaccine coverage can vary widely between both  
404 vaccines and populations [54, 55]. **Further to this point, there are indica-**  
405 **tions that some disease dynamics, such as meningococcal disease, are in a**  
406 **state of self-evolved criticality in their naturally circulating dynamics (i.e.**  
407 **always close to a critical point) [56].** The impact of ever-present critical dis-  
408 ease dynamics on the detectability of early warning signals of a regime shift  
409 in a socio-epidemiological state require further research. For instance, the  
410 critical disease dynamics could serve to mask early warning signals of socio-  
411 epidemiological regime shifts. This would motivate a search for indicators  
412 that can distinguish the socio-epidemiological signal from the background of  
413 critical disease dynamics.

414 Finally, future research could seek early warnings signals in lag-1 SC  
415 measurements from social networks derived from social media data sources

416 such as Twitter. Lag-1 SC is readily calculated if the sentiment of Twitter  
417 users toward vaccines can be assessed as pro- or anti-vaccine. However, the  
418 Twitter follower network is a directed graph that changes in time, therefore  
419 additional theoretical refinements are necessary. **Moreover, our method as-**  
420 **sumes perfect knowledge of the state of nodes on the social layer, whereas in**  
421 **reality this information is partial. Future work should also explore whether**  
422 **censored data on vaccine opinions changes the reliability of the early warning**  
423 **indicators we explored in this paper. This could be addressed by extended**  
424 **models with a parameter for censoring and a distinction between actual and**  
425 **observed opinion status.**

426 Lag-1 spatial correlation appears to be a robust early warning signal for  
427 predicting regime shifts in vaccine uptake under the conditions we studied,  
428 indicating potential for worthwhile additional study in the context of coupled  
429 behaviour-disease interactions.

## 430 5. Acknowledgments

431 The authors are grateful for helpful comments from the editor and reviewers.  
432 This research was funded by Natural Sciences and Engineering Research  
433 Council of Canada (NSERC) Discovery Grants to MA and CTB.

## 434 6. References

### 435 References

- 436 [1] A. D. Lopez and C. D. Mathers, “Measuring the global burden of dis-  
437 ease and epidemiological transitions: 2002–2030,” *Annals of tropical*  
438 *medicine and parasitology*, 2013.
- 439 [2] S. Murch, “Separating inflammation from speculation in autism,” *The*  
440 *Lancet*, vol. 362, pp. 1498–1499, 2003.
- 441 [3] M. Alazraki, “The autism vaccine fraud: Dr. wakefield’s costly lie to  
442 society,” Dec 2011.
- 443 [4] V. A. Jansen, N. Stollenwerk, H. J. Jensen, M. Ramsay, W. Edmunds,  
444 and C. Rhodes, “Measles outbreaks in a population with declining vac-  
445 cine uptake,” *Science*, vol. 301, no. 5634, pp. 804–804, 2003.

- 446 [5] C. Chen, “Rebellion against the polio vaccine in nigeria: implications  
447 for humanitarian policy,” *African Health Sciences*, vol. 4, pp. 205–207,  
448 2004.
- 449 [6] A. S. Jegede, “What led to the Nigerian boycott of the polio vaccination  
450 campaign?,” *PLoS Med*, vol. 4, 2007.
- 451 [7] N. H. Fiebach and C. M. Viscoli, “Patient acceptance of influenza vacci-  
452 nation,” *The American journal of medicine*, vol. 91, no. 4, pp. 393–400,  
453 1991.
- 454 [8] W. O. Kermack and A. G. McKendrick, “A contribution to the mathe-  
455 matical theory of epidemics,” *Proceedings of the Royal Society of London*  
456 *A: Mathematical, Physical and Engineering Sciences*, vol. 115, no. 772,  
457 pp. 700–721, 1927.
- 458 [9] S. Bansal, B. T. Grenfell, and L. A. Meyers, “When individual behaviour  
459 matters: homogeneous and network models in epidemiology,” *Journal*  
460 *of the Royal Society Interface*, vol. 4, no. 16, pp. 879–891, 2007.
- 461 [10] J. Parker and J. M. Epstein, “A distributed platform for global-scale  
462 agent-based models of disease transmission,” *ACM Transactions on*  
463 *Modeling and Computer Simulation*, vol. 22, no. 1, pp. 1–25, 2011.
- 464 [11] L. B. Shaw and I. B. Schwartz, “Fluctuating epidemics on adaptive  
465 networks,” *Physical Review E*, vol. 77, no. 6, p. 066101, 2008.
- 466 [12] A. Perisic and C. T. Bauch, “Social contact networks and disease  
467 eradicability under voluntary vaccination,” *PLoS Comput Biol*, vol. 5,  
468 p. e1000280, 02 2009.
- 469 [13] F. Fu, D. I. Rosenbloom, L. Wang, and M. A. Nowak, “Imitation dy-  
470 namics of vaccination behaviour on social networks,” *Proceedings of*  
471 *the Royal Society of London B: Biological Sciences*, vol. 278, no. 1702,  
472 pp. 42–49, 2011.
- 473 [14] S. Funk, E. Gilad, C. Watkins, and V. A. Jansen, “The spread of aware-  
474 ness and its impact on epidemic outbreaks,” *Proceedings of the National*  
475 *Academy of Sciences*, vol. 106, no. 16, pp. 6872–6877, 2009.

- 476 [15] H.-F. Zhang, Z.-X. Wu, M. Tang, and Y.-C. Lai, “Effects of behav-  
477 ioral response and vaccination policy on epidemic spreading-an approach  
478 based on evolutionary-game dynamics,” *Scientific reports*, vol. 4, 2014.
- 479 [16] W.-X. Wang, Y.-C. Lai, and C. Grebogi, “Effect of epidemic spreading  
480 on species coexistence in spatial rock-paper-scissors games,” *Phys. Rev.*  
481 *E*, vol. 81, p. 046113, Apr 2010.
- 482 [17] A. Perisic and C. T. Bauch, “A simulation analysis to characterize the  
483 dynamics of vaccinating behaviour on contact networks,” *BMC Infec-*  
484 *tious Diseases*, vol. 9, no. 1, p. 1, 2009.
- 485 [18] Z. Wang, M. A. Andrews, Z.-X. Wu, L. Wang, and C. T. Bauch,  
486 “Coupled disease-behavior dynamics on complex networks: A review,”  
487 *Physics of Life Reviews*, vol. 15, pp. 1–29, 2015.
- 488 [19] E. P. Fenichel, C. Castillo-Chavez, M. G. Ceddia, G. Chowell, P. A. G.  
489 Parra, G. J. Hickling, G. Holloway, R. Horan, B. Morin, C. Perrings,  
490 and et al., “Adaptive human behavior in epidemiological models,” *Pro-*  
491 *ceedings of the National Academy of Sciences*, vol. 108, pp. 6306–6311,  
492 Apr 2011.
- 493 [20] C. T. Bauch and A. P. Galvani, “Social factors in epidemiology,” *Science*,  
494 vol. 342, no. 6154, pp. 47–49, 2013.
- 495 [21] C. Granell, S. Gómez, and A. Arenas, “Dynamical interplay between  
496 awareness and epidemic spreading in multiplex networks,” *Phys. Rev.*  
497 *Lett.*, vol. 111, p. 128701, Sep 2013.
- 498 [22] L. Mao and Y. Yang, “Coupling infectious diseases, human preventive  
499 behavior, and networks - a conceptual framework for epidemic model-  
500 ing,” *Social Science and Medicine*, vol. 74, pp. 167–175.
- 501 [23] C. Innes, M. Anand, and C. T. Bauch, “The impact of human-  
502 environment interactions on the stability of forest-grassland mosaic  
503 ecosystems,” *Scientific reports*, vol. 3, p. 2689, 2013.
- 504 [24] L.-A. Barlow, J. Cecile, C. T. Bauch, and M. Anand, “Modelling in-  
505 teractions between forest pest invasions and human decisions regarding  
506 firewood transport restrictions,” *PLoS One*, vol. 9, no. 4, p. e90511,  
507 2014.

- 508 [25] K. A. Henderson, C. T. Bauch, and M. Anand, “Alternative stable states  
509 and the sustainability of forests, grasslands, and agriculture,” *Proceed-*  
510 *ings of the National Academy of Sciences*, vol. 113, no. 51, pp. 14552–  
511 14559, 2016.
- 512 [26] R. P. Sigdel, M. Anand, and C. T. Bauch, “Competition between in-  
513 junctive social norms and conservation priorities gives rise to complex  
514 dynamics in a model of forest growth and opinion dynamics,” *Journal*  
515 *of theoretical biology*, vol. 432, pp. 132–140, 2017.
- 516 [27] Q. Guo, X. Jiang, Y. Lei, M. Li, Y. Ma, and Z. Zheng, “Two-stage ef-  
517 fects of awareness cascade on epidemic spreading in multiplex networks,”  
518 *Phys. Rev. E*, vol. 91, p. 012822, Jan 2015.
- 519 [28] S. Xia and J. Liu, “A computational approach to characterizing the  
520 impact of social influence on individuals vaccination decision making,”  
521 *PLoS ONE*, vol. 8, p. e60373, 04 2013.
- 522 [29] M. Scheffer, J. Bascompte, W. A. Brock, V. Brovkin, S. R. Carpenter,  
523 V. Dakos, H. Held, E. H. V. Nes, M. Rietkerk, and G. Sugihara, “Early-  
524 warning signals for critical transitions,” *Nature*, vol. 461, pp. 53–59,  
525 2009.
- 526 [30] C. T. Bauch, R. Sigdel, J. Pharaon, and M. Anand, “Early warning  
527 signals of regime shifts in coupled human–environment systems,” *Pro-*  
528 *ceedings of the National Academy of Sciences*, p. 201604978, 2016.
- 529 [31] V. Dakos, E. van Nes, R. Donangelo, H. Fort, and M. Scheffer, “Spa-  
530 tial correlation as leading indicator of catastrophic shifts,” *Theoretical*  
531 *Ecology*, vol. 3, no. 3, pp. 163–174, 2010.
- 532 [32] C. Boettiger, N. Ross, and A. Hastings, “Early warning signals: the  
533 charted and uncharted territories,” *Theoretical ecology*, vol. 6, no. 3,  
534 pp. 255–264, 2013.
- 535 [33] M. Scheffer, V. Dakos, and E. H. V. Nes, “Slowing down as an early  
536 warning signal for abrupt climate change,” *IOP Conference Series:*  
537 *Earth and Environmental Science*, vol. 105, pp. 14308 – 14312, 2009.

- 538 [34] C. E. Elger and K. Lehnertz, “Seizure prediction by non-linear time  
539 series analysis of brain electrical activity,” *European Journal of Neuro-*  
540 *science*, vol. 10, pp. 786–789, 1998.
- 541 [35] B. Lebaron, “Some relations between volatility and serial correlations in  
542 stock market returns,” *The Journal of Business*, vol. 65, pp. 199–199,  
543 1992.
- 544 [36] S. R. Carpenter and W. A. Brock, “Early warnings of regime shifts in  
545 spatial dynamics using the discrete fourier transform,” *Ecosphere*, vol. 1,  
546 pp. 2150–8925, 2010.
- 547 [37] T. J. Cline, D. A. Seekell, S. R. Carpenter, M. L. Pace, J. R. Hodg-  
548 son, J. F. Kitchell, and B. C. Weidel, “Early warnings of regime shifts:  
549 evaluation of spatial indicators from a whole-ecosystem experiment,”  
550 *Ecosphere*, vol. 5, no. 8, 2014.
- 551 [38] V. Guttal and C. Jayaprakash, “Spatial variance and spatial skewness:  
552 leading indicators of regime shifts in spatial ecological systems,” *Theo-*  
553 *retical Ecology*, vol. 2, no. 1, pp. 3–12, 2009.
- 554 [39] C. R. Wells, E. Y. Klein, and C. T. Bauch, “Policy resistance undermines  
555 superspreader vaccination strategies for influenza,” *PLoS Comput Biol*,  
556 vol. 9, p. e1002945, 03 2013.
- 557 [40] A. Okabe and K. Sugihara, *Spatial analysis along networks: statistical*  
558 *and computational methods*. Wiley, 2012.
- 559 [41] “Spatial correlation at lag 1,” *Early Warning Signals Toolbox*, 2015.
- 560 [42] S. Kefi, V. Guttal, W. A. Brock, S. R. Carpenter, A. M. Ellison, V. N.  
561 Livina, D. A. Seekell, M. Scheffer, E. H. van Nes, and V. Dakos, “Early  
562 warning signals of ecological transitions: Methods for spatial patterns,”  
563 *PLoS ONE*, vol. 9, p. e92097, 03 2014.
- 564 [43] V. Dakos, S. Kefi, M. Rietkerk, E. H. V. Nes, and M. Scheffer, “Slowing  
565 down in spatially patterned ecosystems at the brink of collapse,” *The*  
566 *American Naturalist*, vol. 177, no. 6, 2011.
- 567 [44] C. T. Bauch and D. J. Earn, “Transients and attractors in epidemics,”  
568 *Proceedings of the Royal Society of London B: Biological Sciences*,  
569 vol. 270, no. 1524, pp. 1573–1578, 2003.



- 570 [45] S. Bansal, B. Pourbohloul, and L. A. Meyers, “A comparative analysis  
571 of influenza vaccination programs,” *PLoS Med*, vol. 3, no. 10, p. e387,  
572 2006.
- 573 [46] A. E. Fiore, D. K. Shay, K. Broder, J. K. Iskander, T. M. Uyeki,  
574 G. Mootrey, J. S. Bresee, and N. J. Cox, “Centers for disease control  
575 and prevention,” Aug 2008.
- 576 [47] D. M. Vickers, A. M. Anonychuk, P. De Wals, N. Demartean, and C. T.  
577 Bauch, “Evaluation of serogroup c and acwy meningococcal vaccine pro-  
578 grams: Projected impact on disease burden according to a stochastic  
579 two-strain dynamic model,” *Vaccine*, vol. 33, no. 1, pp. 268–275, 2015.
- 580 [48] P. Erdos and A. Renyi, “On random graphs,” *Publicationes Mathematicae*,  
581 vol. 6, pp. 290–297, 1959.
- 582 [49] R. Albert and A.-L. Barabasi, “On random graphs,” *Science*, vol. 286,  
583 pp. 509–512, 1999.
- 584 [50] D. Easley and J. Kleinberg, *Networks, crowds, and markets reasoning*  
585 *about a highly connected world*. Cambridge University Press, 2010.
- 586 [51] “Synthetic data products for societal infrastructures and proto-  
587 populations: Data set 1.0,”
- 588 [52] D. Ivaneyko, J. Ilnytskyi, B. Berche, and Y. Holovatch, “Local and  
589 cluster critical dynamics of the 3d random-site ising model,” *Physica A:*  
590 *Statistical Mechanics and its Applications*, vol. 370, no. 2, pp. 163–178,  
591 2006.
- 592 [53] J. Dushoff, J. B. Plotkin, S. A. Levin, and D. J. Earn, “Dynamical res-  
593 onance can account for seasonality of influenza epidemics,” *Proceedings*  
594 *of the National Academy of Sciences of the United States of America*,  
595 vol. 101, no. 48, pp. 16915–16916, 2004.
- 596 [54] T. A. e. a. Santibanez, “Flu vaccination coverage, united states, 2014-15  
597 influenza season,” 2015.
- 598 [55] L. D. Elam-Evans, D. Yankey, J. Singleton, and M. Kolasa, “National,  
599 state, and selected local area vaccination coverage among children aged  
600 19-35 months, United States, 2013,” 2014.

- 601 [56] N. Stollenwerk, M. C. Maiden, and V. A. Jansen, “Diversity in  
602 pathogenicity can cause outbreaks of meningococcal disease,” *Proceed-*  
603 *ings of the National Academy of Sciences of the United States of Amer-*  
604 *ica*, vol. 101, no. 27, pp. 10229–10234, 2004.

ACCEPTED MANUSCRIPT